

Digital Twin Development of a Testing Grid Using a Grid Analyzer

DERK GONSCHOR ^{1,2}, JONAS STEFFEN ¹, JUAN ALVARO MONTOYA PEREZ ¹, CHRISTIAN BENDFELD ¹,
DETLEF NAUNDORF³, PHILIPP KOST³, CHRISTIAN AIGNER³, FLORIAN FÜLLGRAF ¹, RON BRANDL^{1,2},
AND MARCO JUNG ^{1,2} (Senior Member, IEEE)

¹Department Converter and Drive Technology, Fraunhofer IEE, 34117 Kassel, Germany

²Hochschule Bonn-Rhein-Sieg University of Applied Sciences, 53754 Sankt Augustin, Germany

³Department Testing Solutions, MicroNova AG, 85256 Vierkirchen, Germany

CORRESPONDING AUTHOR: DERK GONSCHOR (e-mail: derk.gonschor@h-brs.de)

This work was supported in part the German Federal Ministry for Economic Affairs and Climate Action and in part by the Project Coordinator Jülich for funding the Research Project *CoMap* under Grant 03EI6080B.

ABSTRACT The recent transformation of the energy sector brings new challenges in areas such as supply security, efficiency, and reliability. Especially the increase of decentralized power plants leads to a more complex energy system and an increasing complexity. This requires expansion and digitization of the power grid as well as an initiative-taking operation of the grid operator. To investigate such complex systems and its phenomena, modern development methods such as real-time simulation or digital twins (DT) can be used. In this approach a digital replica of the real-world system, a grid section, is developed, which can represent or predict the behavior of the real distribution grid. For this, a model of the real-world system is derived and implemented in a co-simulation environment, in which it receives data via an analyzer or measurement system from the grid model. This paper focuses on the development of the digital twin of a testing grid and a grid analyzer for the measurement. With the digital twin of the testing grid, a first approach is achieved in a real-time capable environment showing the functionalities and interactions of a digital twin. Subsequently the development of the digital twin model is explained, and the results are discussed.

INDEX TERMS Digital twin, real time systems, power system simulation, signal analysis, power system measurements, power system state estimation.

I. INTRODUCTION

A. MOTIVATION

The exclusive consideration of individual consumers, such as heat pumps, factories, or residential structures, is proving to be insufficient in view of the increasing integration of Distributed Energy Resources (DERs). To comprehensively analyze the electrical energy system and assess the current state of distribution grids, the increasing use of measurement sensors within the distribution infrastructure, combined with observations, is essential. Innovative development methods such as real-time simulations (RTS) and, in particular, digital twins (DTs), represents novel frameworks for the modeling of complex systems and its dynamics. These simulations enable the emulation of load flows in specific grid sections and facilitate the execution of predictive analysis [1]. The presented

DT observes a distribution grid, which will be simulated in real-time and in parallel to the real distribution grid. The DT receives actual measured data from multiple grid analyzers (GAs) integrated in the real system. This creates a virtual environment as realistic as possible and can detect missing data gaps, e.g., unknown loads flows. In addition, the use of DTs can significantly reduce the number of metering systems in the grid, as many data gaps are captured by the model. The aim of the digital twin of a grid section is to increase the ability to observe the section and lowering the costs for the grid operator through the saving of measuring points [1], [2], [3].

For the realization of a DT, the model of the distribution grid itself, the GA and their connection have to be developed. In contribution to this, the software of a GA has been developed in [4] and the results have been presented in [5].

The purpose of this paper is to show further work, focusing more on the development of the DT and the integration of the GA.

B. STATE OF THE ART

DT is a new framework to analyze and solve existing and new phenomena in complex systems. However, recent advances in information technology have enabled more feasible and practical DT implementations. For this reason, the topic of DT has gained more attention in recent years. In the context of electrical energy systems, the focus lied more upon other innovative development methods, such as RTS as well as Co-Simulation or Hardware-in-the-Loop (HiL) which are present in research and development for around ten years [6], [7], [8]. However, these are momentary studies in which individual predefined scenarios are used in simulations or laboratories. The use of real-time systems and co-simulation platforms for high-performance continuous operation to achieve a continuous digital image of grid model operations has only been used occasionally in research to date [2], [3], [9], [17].

II. INNOVATIVE DEVELOPMENT METHODS

A. SIMULATION METHODS

Over the past three decades, advancements in simulation technology have enabled the execution of more complex and faster simulations [6], [7] as well as the use of smaller time steps. This allows a more detailed and deeper analysis of different systems and distinguishes which phenomena can be investigated. In case of electrical grids, if for example the stability is the goal of the investigation, a time step of one second can be enough, while for transient switching operations, around 100 μ s are used. Depending on the simulation time step, there are also varying methods to perform the calculation and a fitting method must be chosen depending on the goal of the simulation. For the analysis of electrical networks and grids, the simulation with electromagnetic sub-transient signals (EMT) or electro-mechanical (RMS / Phasor) simulation are suitable. Here, phasor simulations are used for time steps greater than 1 ms and EMT simulations are used for faster time steps [10], [11].

B. REAL-TIME SIMULATION

Achieving RTS is contingent upon ensuring that the simulation time corresponds to real-time. Consequently, the execution time (T_e) for each step must be less than or equal to the time step (t_n). Failure to meet this criterion results in an overrun, precluding the attainment of real-time simulation. Conversely, if the execution time (T_e) is less than the time step (t_n), the execution of the following time step ($T_e(n+1)$) is paused until the initiation of the next time step (t_{n+1}), leading to idle time. Fig. 1 illustrates the three different aforementioned simulation types: non-RTS which executes with its own computation time without regard to real time; RTS with idle time which executes synchronized with real time; and RTS with overruns which computation time could seldom exceed the real time [12]. In the context of electrical components,

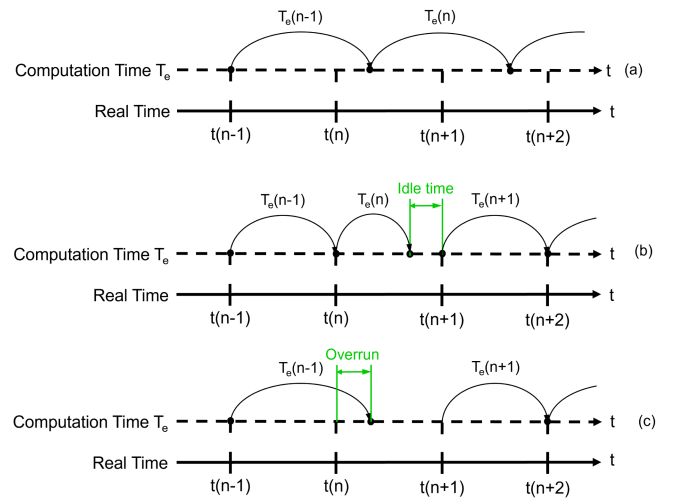


FIGURE 1. Comparison of different simulation methods: (a) fixed-step non-real-time simulation, (b) real-time simulation with idle time, and (c) real-time simulation with overrun based on [12].

particularly power electronics, the selection of a time step is critical to accurately generate voltage and current wave forms while ensuring the computer can solve the equations within the designated time step [12], [13].

For RTS, the simulation method is also an essential part, since the simulation methods have an impact on the computing power and thus, the execution time and the fulfillment of the real-time criteria. In general, RTS is used for the simulation of detailed analysis and investigating current and voltage wave forms. Therefore, for RTS EMT simulations with a time step of 50 μ s are used in general [13].

C. CO-SIMULATION

In classical simulation, one model and one solution method are used to solve the equation of the model. This self-contained environment is the basic approach, but there are use cases where it is useful, for example, to split the model into different sub-models or to use multiple simulation environments. Depending on whether the model is separated or multiple solution methods are used for simulation, there are different definitions for these simulation types. The simulation types are discussed in more detail below on the basis of [8], [14], [15]:

- **Parallel simulation**: Here, a model is modeled in one simulation environment and divided into several domains. This can result in multiple solution methods or different time steps for the respective domain. However, this is still referred to as “closed modeling”, but “distributed simulation”.
- **Hybrid simulation**: If the original model is separated into several sub-models, but these can still be solved using a single solution method or combined in a formula, this results in a “closed simulation” and “distributed modeling”.
- **Co-simulation**: The use of multiple models and multiple solution methods results in “distributed modeling”

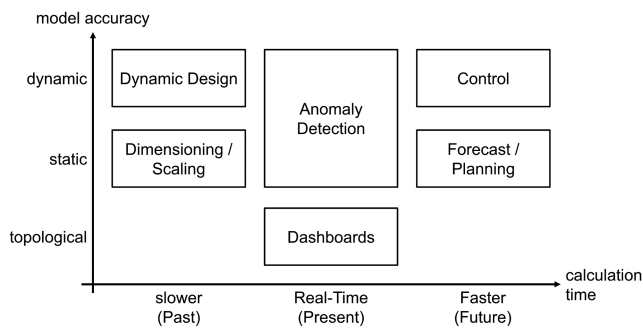


FIGURE 2. Application of different variants of digital twins depending on the calculation time and model accuracy based on [1].

and “distributed simulation”. These must be coupled by exchanging data or information between the two simulations. This is therefore referred to as a “coupled simulation” or a “co-simulation”.

D. DIGITAL TWINS

The word Digital Twin is currently used in many different contexts and the definition changes continuously [9], [16]. In 2012, the word DT was first defined as a simulation of a vehicle or system in its actual state that uses physical models, sensors, etc. to reflect the behavior of the associated real twin (here the real vehicle) [18]. In the last 12 years, many definitions were added, as [19] shows. Accordingly, a DT is a computerized model of a physical system that shows all the functions and connections of the physical system. These definitions, however, assume a static model that is not supported or fed by real data from the physical system. This approach is added in [20]. Here, the static model is transformed and becomes a living or dynamic model that is continuously adapted to changes. From the authors perspective, the main DT core function is to host a computer program or model that uses data from the real world to present and/or predict the behavior of a product or process. This distinguishes a DT from a pure or digital model through the automatic exchange of data between the physical system or process and the digital twin. This means that a change in the physical system or process in the digital model has no effect on the model itself, whereas in the DT, a change of state in the physical system always results in a change of state in the digital twin [9].

DTs can be divided into two main categories depending on the application. These are based on the system that is to be digitally replicated. When digitally replicating the energy market, a supply or production chain, it is called a DT of an economic, business or social object or process. However, if DTs are created of a physical object, such as an engine, a wind turbine or entire cities, this is referred to as a digital representation of a physical object [21].

The use of digital twins depends mainly on the accuracy of the model and its calculation time or time step [1], as Fig. 2 shows. When developing the DT of an electrical (distribution) grid, the depth and the accuracy of the model must be given special consideration, since large grid models have a huge

computation expense. Depending on the model accuracy and the computation time, there are many applications for DTs in the context of the electrical energy system. The following list shows a selection based on [1], [2], [3]:

- Advice in the control room: DTs can help support the professional judgment of grid operators when they need to make quick decisions to ensure a reliable power supply.
- Post-Mortem Analysis: Analyzing past events in the power grid and identifying faults or anomalies by looking for causalities and ramifications.
- Long-term decision support: assessing the feasibility of alternatives and investigating solutions.
- Asset Management: predictive maintenance of circuit breakers, components, etc. through high model accuracy and model depth of a DT.
- Cyber-Physical-System (CPS): DT could enable seamless integration between the cyber and physical space instead of modeling the existing CPS as a whole system, which is the focus of current CPS research.
- Artificial Intelligence (AI): Novel digital trends such as AI, machine learning (ML), or reinforcement learning (RL) can help with modeling DTs as well as anomaly detection or prediction.
- Future Scenarios: Simulation of future events taking into account real and current data.

III. GRID ANALYZER

To realize a digital twin, real data of the observed real system is needed. To establish a digital twin of a grid section, a unit for recording measured values is required, referred to below as a GA. The GA comprises the measurement system for recording the data and the analysis function for interpreting the measurement data. Furthermore, the data processing and the communication connection to the real-time system is an important component, especially in the context of grid analyses as the measuring points, or grid nodes of interest, have a wide regional distribution.

A. MEASUREMENT SYSTEM

A digital twin imposes special requirements on the measuring system, whereby the requirements vary for different applications. To be able to cover as many applications as possible with the measuring system, in addition to the grid analysis scenario, the measuring circuit was developed to meet various requirements. Table 1 shows a section of the specification. In order to be able to react flexibly to different measurement applications, the analyzer is implemented with a variable measuring card slot system that can accommodate up to 8 measuring cards. Furthermore, an SoC-FPGA is used as the central processing unit to enable flexible measurement card connection with different sampling rates and analogue-to-digital converters. The system can cover a wide range of communication interfaces; the UDP connection is particularly interesting when used for digital twins of distribution grids. Also enables via the FPGA high-speed DT applications with

TABLE 1. Specification of the Developed Measurement System

Main system	
Description	Specification
System structure	Flexible plug-in card design 8 slots
Processing unit	SoC-FPGA with ARM core
Communication interfaces transfer rate ≤ 1 kHz	UDP, TCP, Modbus
High-speed communication interface transfer rate $\gg 1$ kHz	Fibre optics with aurora protocol
Maximal sample frequency	75 kHz
Housing form factor	19-inch housing
Measurement card voltage	
Rated measurement range	± 800 V
Number of channels	6
Desired Accuracy	8 V
Measurement card current	
Rated measurement range	± 8 A
Number of channels	6
Desired Accuracy	80 mA

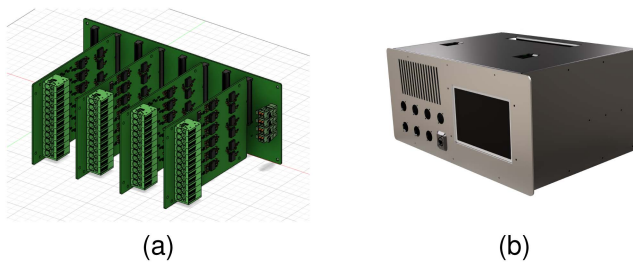


FIGURE 3. Grid analyzer (a) multi-card system and (b) 19-inch housing.

sample frequencies over several hundred kilohertz with the high-speed Ethernet channels. The setup is integrated in a 19-inch housing. Fig. 3 shows the multi-card system and the housing of the GA.

Each voltage measurement card comprises six measurement channels, each is designed to work in a grid with phase-to-ground voltages of 230 V as input voltage. Each current measuring card also provides six measuring channels and uses a shunt resistor to measure the current. A maximum value of 8 A can be recorded with the current measurement. Delta-sigma converters are used for the analog-to-digital conversion and the FPGA is used to reconstruct the measured signal from the over-sampled bit-stream [40]. The measurement cards are shown in Fig. 4.

Fig. 5 shows the measured current with a sinusoidal profile. The red curve represents the current recorded by the GA, while the black curve shows the reference measurement with an oscilloscope. The current of the developed measurement system and the reference measurement are congruent in terms of time and amplitude. When commissioning the measuring circuits, the measuring error was determined over the measuring range at different temperatures. At a temperature of 60 °C, the largest measurement error of 80.39 mA was determined for the current at 8 A, which is slightly above the permissible value of 80 mA. At the same temperature point, the largest measurement error of 519.99 mV was found for the voltage measurement at the measurement point 800 V, which is well

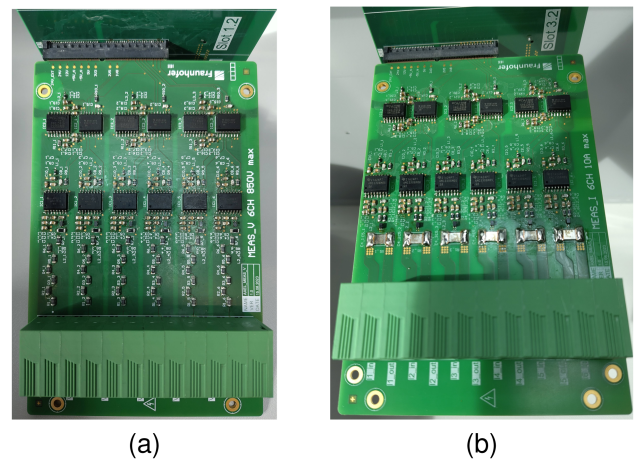


FIGURE 4. Picture of the measurement cards (a) voltage and (b) current.

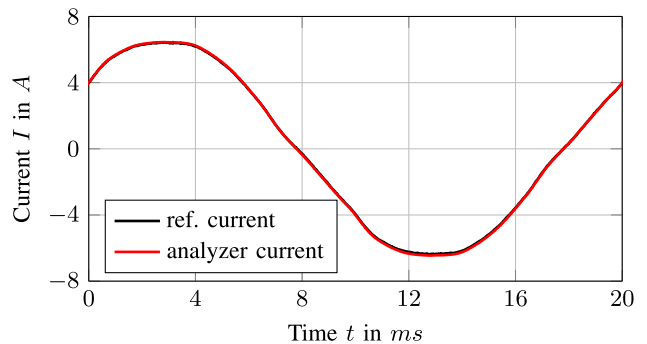


FIGURE 5. Example of a current measurement with a comparison to a reference measurement.

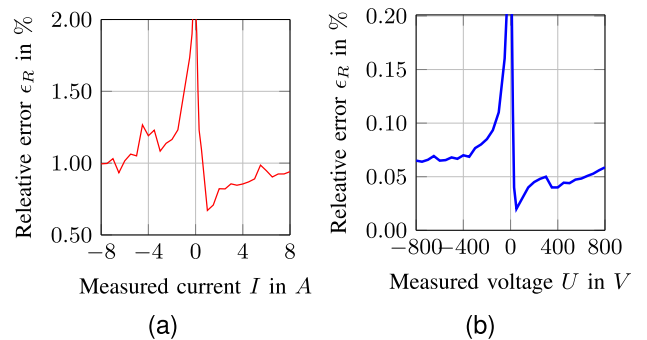


FIGURE 6. Error chart of the measurement of (a) current and (b) voltage.

below the permissible deviation of 8 V. Despite the very slight exceeding of the maximum measurement deviation for the current measurement, the GA is suitable for the measurement tasks as part of the digital twin. Fig. 6 shows the recorded relative error chart for voltage and current within the measuring range. When analyzing the relative error, the range around zero was not considered as this, by definition, becomes infinite when calculating the relative error. For the current, the relative error lies in a range of 0.67% to 1.73% for the recording of the positive current, a slightly increased deviation results. The

TABLE 2. Dependency of the Analysis Functions

Characteristics	Independent	DSOGI-FPLL	FFT
Amplitude for each Harmonic	-	-	X
Phase for each Harmonic	-	-	X
Frequency and Phase Angle	-	X	-
Power	X	X	X
Asymmetry	X	X	X
Total Harmonic Distortion	-	-	X
Distortion Reactive Power	-	-	X
Distortion Factor	-	-	X
Power Factor	-	-	X
Root-Mean-Square values	X	X	-

voltage measurement shows a range of 0.02% to 0.16% for the relative error and thus has a very low deviation compared to the current. Furthermore, the relative error for current and voltage is subject to small fluctuations and only shows the sharp increase characteristic of the relative error when the measured value reaches zero.

The analyzer can measure low-voltage values. However, the area of application is not only the low-voltage but also the medium-voltage grid. In addition to the low-voltage grid, it can also be used in the medium-voltage grid. To be capable of using the measuring system for medium voltage, measuring transformers are used to convert the voltage and current values from the distribution grid to match the input range of the grid analyzer. The use of frequency-optimized medium-voltage current and voltage transformers are planned for the system.

B. ANALYSIS FUNCTIONS

The analysis functions are used to calculate certain parameters of current and voltage to visualize grid phenomena such as harmonics or distortions of nominal values. The functions have been developed in accordance with the state of the art. As a development tool, *Matlab Simulink* has been used.

The analysis functions include a lot of functions. However, the two main functions are the Fast-Fourier-Transformation (FFT) and the combination of the so called double second-order generalized integrator (DSOGI), and a frequency- and phase-locked-loop (FPLL), resulting on a DSOGI-FPLL. The other functions are based on the results on one of these functions, as Table 2 shows.

Here, the two main functions are explained in more detail.

1) FAST FOURIER TRANSFORMATION

The goal of the FFT is the harmonic analysis of a periodic signal. Therefore, it is considered in the frequency domain and not in the time domain. Here, the signal can be analyzed on a larger scale. For discrete simulations, the Discrete Fourier Transformation (DFT) is used, where instead of a continuous signal, its discretized version is used and multiplied by the Euler equation:

$$X(k) = \frac{1}{N} \sum_{n=0}^{N-1} x(n)e^{-j(2\pi n/N)k}; k = 0, 2, \dots, N - 1 \quad (1)$$

TABLE 3. Parameters of the DSOGI-FPLL Based on [5]

Abbreviation according to Figure 7	Description	Value
ω_n	Nominal frequency	314.16 1/sec
k	Proportional Factor in DSOGI	1.8
k_{FLL}	Adjustment of Amplitude in FLL	0.25
k_f	Adjustment Error in FLL	-2
p_{FLL}	Proportional Factor in FLL	-10
K_n	Adjustment q -component in PLL	0.2
P, I	P and I Factor in PLL	[200 800]
p_{PLL}	Proportional Factor in PLL	-1

Here, $x(n)$ is the periodic signal to be analyzed, N are the number of discrete sample points, $X(k)$ the converted signal in the frequency domain and the frequency resolution of k can be defined as the ratio of sampling frequency over number of discrete sample points f_s/N . For the implementation done here, a sampling frequency of 5.12 kHz and 1024 sample points have been defined. With this boundary condition and due to the symmetry properties of the DFT, a spectrum with values between zero and 2.5 kHz with a step size of 5 Hz are obtained. For the implementation of the DFT, *Matlab's fft* function [22] is used, since it uses an optimized calculation method while having similar results.

2) DSOGI-FPLL

For primarily calculating the grid frequency and the phase angle, this work uses an analysis which consists of the three core building blocks of a Quadrature-Signal Generator (QSG), a Positive- and Negative-Sequence Calculator (PNSC), and finally a Frequency-Locked Loop (FLL) in combination with a Phase-Locked Loop (PLL). The development of the core building blocks has been based on [23], [24], [25], [26]. In general, in the QSG the sine waves are filtered to reduce the harmonics and in the PNSC, the positive and negative sequence are calculated based on the filtered signal. After that, a combination of a PLL and a FLL is used to calculate two frequency errors, which are added to the nominal frequency. Through integration of the calculated frequency, the phase angle can be determined. Fig. 7 visualizes the schematic overview of the DSOGI-FPLL, while Table 3 shows its parameter values.

C. COMMUNICATION INTERFACE

The measurements of the GA and the calculated values previously described are sent to the DT of the distribution grid later in the conversion. For the DT to receive the real-time data, the GA must work in real time. This requires that the system calculates the results in real time and sends these results to the DT with a real-time capable interface.

The capability of the communication interface is depending on how much data can be transferred from the GA to the DT. The real-time capability is also limited depending on the distance, as the maximum speed at which both digital and analog signals can be transported is the speed of light. Real-time capability therefore decreases with increasing distance.

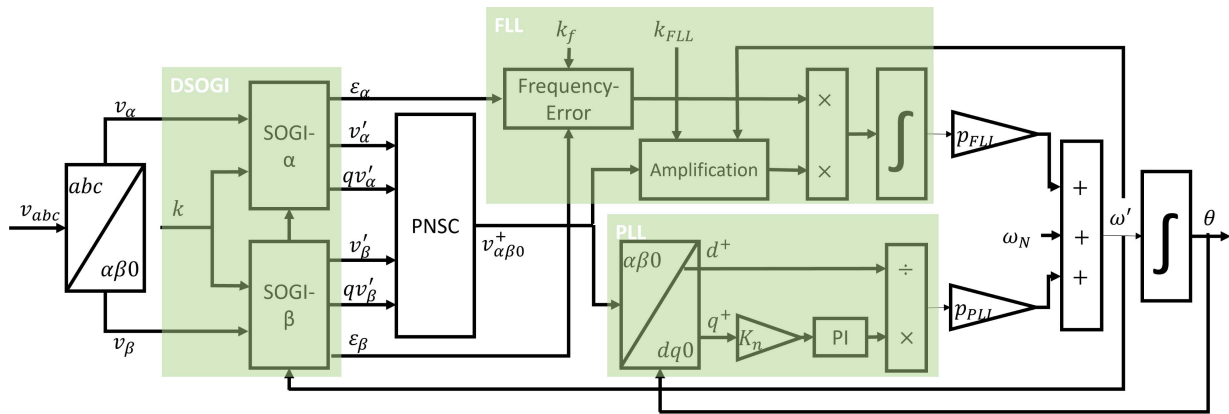


FIGURE 7. Schematic overview of the DSOGI-FPLL based on [5].

For a real-time capable exchange of data via a digital interface, the two systems (GA and DT) must be synchronized, similar as with an RTS. This ensures that the GA and the DT are synchronized to the same time. Unlike with analogue interfaces, this must be achieved using a synchronization process. On the other hand, a real-time capable communication protocol is required so that the data can be sent from one device to the other in real time.

1) SYNCHRONIZATION PROCESS

As described in the requirements, the clocks of the GA and the DT must be synchronized. To achieve this, each device must have a common time. This can be achieved by integrating quartz timing chips into the devices [27] but is mainly obtained by receiving the time from a third-party device. The common time can for example be realized by radio waves, a Global Positioning System (GPS) satellite and the standardized process C37.118 [28], [29] or the Network Time Protocol (NTP) [30], where the participants are divided into so-called stratum and the time is compared between the levels [31]. However, each synchronization process can entail a number of problems. While the use of quartz timing chips results in high costs, receiving the common time by a third party device can cause time delays [27].

2) COMMUNICATION PROTOCOL

As described in the requirements, the data must be sent via a real-time capable communication protocol. Therefore, Table 4 shows a selection of communication protocols and classifies them according to their real-time capability.

TABLE 4. Real-Time Capability of Different Ethernet-Based Communication Protocols

Communication Protocol	Ref.	Real-Time capability
Transmission Control Protocol (TCP)	[32]	No, reliability guaranty causes latency in data transfer
User Datagram Protocol (UDP)	[32] [33]	No guaranty but higher possibility than TCP
Open Platform Comm. Unif. Architecture (OPC UA)	[32]	Only in combination with other real-time capable protocols
Process Field Net (PROFINET)	[34]	Yes, established in automation
Ethernet Ctrl Automation Technology (EtherCAT)	[35]	Yes, established in automation
Distributed Network Protocol (DNP3)	[36]	Yes, established in electrical energy system

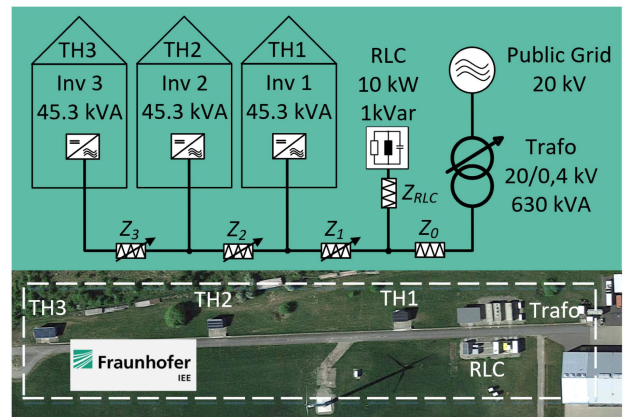


FIGURE 8. Low-voltage smart grid test center SysTec Fraunhofer IEE in Fuldata, Hessen, and Germany.

IV. DIGITAL TWIN OF A GRID SECTION

A. REAL TESTING GRID

A Model is developed based on the Smart Grid Test Center at SysTec [41] as shown in Fig. 8. There is a low-voltage test grid on the test site, within three “test households” TH1-TH3 are connected via cables with different (and variable) impedances $Z_0 - Z_3$, and an additional RLC-Load Bank connected with the cable Z_{RLC} . The test households are fully customizable,

whereby loads and generation can be connected and networked in the entire smart grid. Within the scope of this investigation, a PV inverter will be considered and modelled for each test household and due to their geographical position, the same irradiance is assumed.

The electrical properties of the devices in the model are collected in Table 5; and the properties of the selected cables are shown in Table 6, where the subindex 0 represents the zero-sequence impedance and the subindex 1 represents

TABLE 5. Electrical Properties of the Modeled Devices in the Testing Grid

Device	Model Type	Electrical Values
Public Grid	Three-Phase Source	$U_{Base} = 20 \text{ kV L-L}$ $S_{SC} = 100 \text{ MVA}$ $X/R \text{ Ratio} = 9$
Transformer	Three-Phase Transformer	$U_{Pri} = 20 \text{ kV}$ $U_{Sec} = 0.4 \text{ kV}$ $S_n = 630 \text{ kVA}$
PV Inverter	I Source with dq control and PQ Set-points	$S_{max} = 43.5 \text{ kVA @ } 1000 \text{ W/m}^2$ Irradiance profile as input
RLC Bank	Three-Phase Series RLC Load	$P = 10 \text{ kW}$ $Q = 1 \text{ kVAr}$

TABLE 6. Electrical Properties of the Cables in the Testing Grid

PI Section Line	Resistance in Ω/km	Inductance in mH/km	Capacitance in nF/km
Z_0 Length 0.1 km	$R_0 = 0.5$ $R_1 = 0.125$	$L_0 = 1.02$ $L_1 = 0.254$	$C_0 = 422$ $C_1 = 870$
Z_1 Length 0.3 km	$R_0 = 2.565$ $R_1 = 0.642$	$L_0 = 1.080$ $L_1 = 0.270$	$C_0 = 276$ $C_1 = 670$
Z_2 Length 0.6 km	$R_0 = 1.777$ $R_1 = 0.444$	$L_0 = 1.050$ $L_1 = 0.270$	$C_0 = 312$ $C_1 = 750$
Z_3 Length 0.6 km	$R_0 = 1.017$ $R_1 = 0.254$	$L_0 = 1.020$ $L_1 = 0.256$	$C_0 = 386$ $C_1 = 840$
Z_{RLC} Length 0.2 km	$R_0 = 1.017$ $R_1 = 0.254$	$L_0 = 1.020$ $L_1 = 0.256$	$C_0 = 386$ $C_1 = 840$

the positive-sequence impedance. The grid section described will be developed as a digital twin. Initially, the model undergoes simulation-based investigations, which guide the subsequent integration and placement of GAs within the grid section.

B. REAL TIME SYSTEM

The real-time simulation system *NovaCartis* from *MicroNova* is used as simulation platform. The computer architecture is based on a real-time computer, which is called simulation node, and a standard *Windows* PC for operating and configuring the system. The simulation nodes work with a Linux-based real-time operating system. Depending on the number of grid nodes to be calculated, simulation nodes can be selected in different performance classes. There is a choice of quad-core or octo-core processors. In the High-Performance Parallel Simulation Node, 12 processors work in parallel. In addition, clusters of several simulation nodes can be set up. The individual nodes are coupled via the *NovaCartis* real-time Ethernet. The same protocol is used to integrate the *NovaCartis* interface boards for connecting special hardware, like the GA. The measurement systems can be connected via Ethernet UDP and Modbus via TCP/IP. A CPU isolation function allows sampling times for partial models of up to 20 μs . Grid models can be integrated directly from *Matlab Simulink* into the real-time system via the *NovaCartis* tool chain. *NovaCartis* also supports the Functional Mockup Interface (FMI) for co-simulation for distributed modeling and distributed simulation [39].

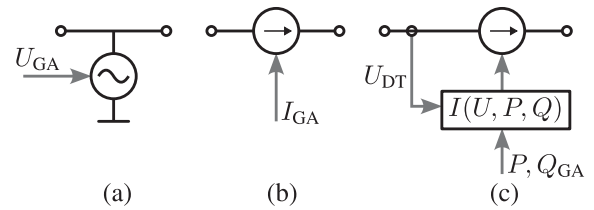


FIGURE 9. Grid Analyzer model coupling: (a) $U(u)$. (b) $I(i)$. (c) $I(u,p,q)$.

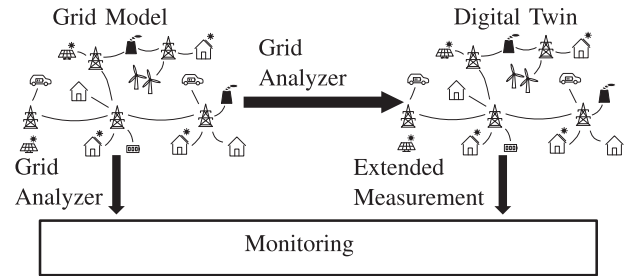


FIGURE 10. Simulation of the digital twin.

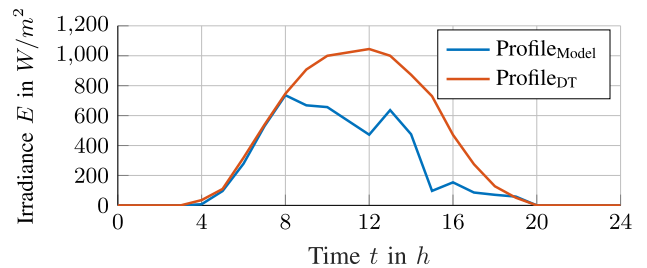


FIGURE 11. Profile of the PV irradiance for simulation and the digital twin.

C. DIGITAL TWIN OF THE TESTING GRID

In a first step, the grid described in Section IV-A is modelled in *Matlab Simulink*. For the present work, the simulation type is set to phasor, so that the model can also be operated efficiently for complex distribution grids. The three-phase PI section line models from the *Simulink* library are used for modeling the cables in the test grid. To realize the model as a digital twin, the measured voltages and currents of the GAs must be reproduced at the corresponding nodes. As this is a simulation, no data loss can occur. However, this must be considered in the field test. Hence, the measured values are held by the grid analyzer model until updated measured values are received. This is possible since the digital twin is calculated as a phasor simulation and only works with RMS values. After a certain time, e.g., two sample time steps, without updating the measured values, a warning must be issued and the model is no longer valid.

The fact that the measured values are fed in directly ensures that the DT works at the same operating point at the connection point. Fig. 9 shows the three methods of coupling used to influence the state of the DT with the measured values on the node:

- U Source with U Magnitude $U(u)$ (Fig. 9(a)): A programmable voltage source is connected and is controlled

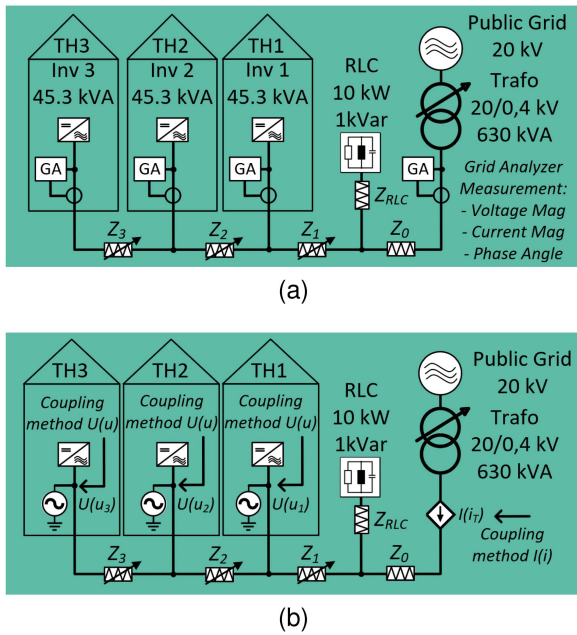


FIGURE 12. Node case $U_3 - I_1$: (a) Placement of the grid analyzer in the real model and (b) Integration of the coupling methods for the digital twin.

by the measured voltage magnitude. In the DT, the voltage at the connection point of the grid analyzer is ideally simulated.

- *I Source with I Magnitude $I(i)$* (Fig. 9(b)): A programmable current source is connected and is controlled by the measured current magnitude. In the DT, the current at the connection point of the grid analyzer is ideally simulated.
- *I Source with P and Q balance $I(u,p,q)$* (Fig. 9(c)): A programmable current source is connected and is controlled by the measured active and reactive power from the grid analyzer and the measured voltage in the DT. In the DT, the active and reactive power at the connection point of the grid analyzer is ideally simulated.

D. SIMULATION

The developed model from Section IV and its DT are implemented as a *Matlab Simulink* model. The basic principle of the simulation is depicted in Fig. 10. The DT is simulated and the GA is used to acquire data from the grid model.

In order to analyze the impact of the GAs on the DT, both the test grid model and the digital twin are implemented and simulated in the RTS. The DT is designed to mirror the test grid model, incorporating the coupling methods described in Section IV-C.

Two different PV irradiance profiles are used for the model, taken from the hourly radiation data available in [37] and presented in Fig. 11.

For the model the irradiance profile at June 8th, 2020 is used, while for the DT model the date June 2nd, 2020 is taken. The coordinates Latitude 51.389, Longitude 9.515 are included in the PVGIS-SARAH2 database, and a slope of 40°

TABLE 7. Node Cases: Placement of Grid Analyzers in Models

Node Case	Trafo	TH1	TH2	TH3
w/o GA	x	x	x	x
U_1	x	$U(u)$	x	x
U_2	x	$U(u)$	$U(u)$	x
U_3	x	$U(u)$	$U(u)$	$U(u)$
$U_3 - I_1$	$I(i)$	$U(u)$	$U(u)$	$U(u)$
PQ_1	x	$I(u,p,q)$	x	x
PQ_2	x	$I(u,p,q)$	$I(u,p,q)$	x
PQ_3	x	$I(u,p,q)$	$I(u,p,q)$	$I(u,p,q)$
PQ_4	$I(u,p,q)$	$I(u,p,q)$	$I(u,p,q)$	$I(u,p,q)$

and an azimuth of -5° are assumed to generate the profiles. The two different profiles ensure a disturbance which define different stable points in each system. Different PV profiles were selected as this represents a large unpredictable deviation between the grid model and the DT. This approach is used to demonstrate that a GA would minimize the error due to random disturbances or false parameterization.

The analysis will be focused on 4 nodes: low-voltage side of the transformer and each point of connection from the test houses TH1, TH2 and TH3; therefore, GAs are placed in this nodes of interest in the real model in order to be monitored and to provide information to the DT as shown in Fig. 12.

Taken into account these 4 nodes and the 3 methods of coupling defined in Section IV-C, 9 out of 256 possible combinations of GA arrangements are implemented as condensed in Table 7.

The node case $U_3 - I_1$ is shown as a reference in Fig. 12. The voltages u_{1-3} are taken at the measurement points TH1, TH2 and TH3 and $U(u)$ is used as the coupling method to feed the reference variable from the model into the DT, while the coupling method $I(i)$ is used for the transformer measuring point and the current i_T is being fed in. The Fig. 12(b) shows the possibility to use different coupling methods in one digital twin model.

E. SIMULATION RESULTS

The analysis of the simulation results is at first performed graphically by comparing the curves of voltage, current and angle between them (ϕ), for each of the node cases presented in Table 7. Fig. 13 presents the comparison on the data in TH1 between the DT node cases w/o GA, $U_3 - I_1$, PQ_3 against the model. Due to the dynamical behavior of the error, the Root Mean Squared Error (RMSE) is used additional as a metric for the model deviations as presented in (2) [42], where y is the measured data from the model and \hat{y} is the DT extended measurement. The Relative RMSE (RRMSE) defined in (3) is used to represent the values in percentage where $\bar{\hat{y}}$ represents the mean value of \hat{y} .

$$RMSE(y, \hat{y}) = \sqrt{\frac{\sum_{i=1}^N (y_i - \hat{y}_i)^2}{N}} \quad (2)$$

$$RRMSE(y, \hat{y}) = \frac{RMSE(y, \hat{y})}{\bar{\hat{y}}} \quad (3)$$

TABLE 8. Calculated RRMSE of the Simulations Results

	Node	no GA	U_1	U_2	U_3	$U_3 - I_1$	PQ_1	PQ_2	PQ_3	PQ_4
U_{Mag}	Trafo	0,15%	0,16%	0,17%	0,17%	0,11%	0,11%	0,08%	0,05%	0,01%
	TH1	3,20%	0,17%	0,07%	0,07%	0,43%	2,42%	1,72%	1,01%	0,98%
	TH2	5,52%	2,87%	0,11%	0,06%	0,07%	4,83%	3,32%	1,76%	1,74%
	TH3	6,15%	3,61%	0,96%	0,06%	0,06%	5,49%	4,03%	1,97%	1,95%
I_{Mag}	Trafo	62,91%	3,40%	4,41%	4,54%	0,00%	52,06%	40,45%	26,12%	8,51%
	TH1	60,39%	>100%	11,27%	8,68%	>100%	22,48%	23,52%	24,58%	24,62%
	TH2	58,11%	61,57%	98,93%	1,41%	26,81%	59,01%	21,68%	23,90%	23,94%
	TH3	57,48%	60,79%	64,27%	3,45%	5,01%	58,34%	60,23%	23,70%	23,73%
Angle ϕ	Trafo	25,12%	55,11%	65,48%	67,03%	>100%	23,22%	20,75%	16,66%	8,41%
	TH1	2,20%	>100%	40,34%	34,95%	>100%	1,30%	1,30%	1,30%	1,30%
	TH2	2,32%	2,32%	>100%	30,75%	>100%	2,32%	1,48%	1,48%	1,48%
	TH3	2,20%	2,20%	2,20%	36,50%	>100%	2,20%	2,20%	1,30%	1,30%

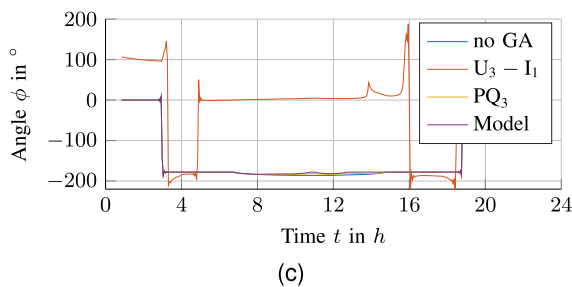
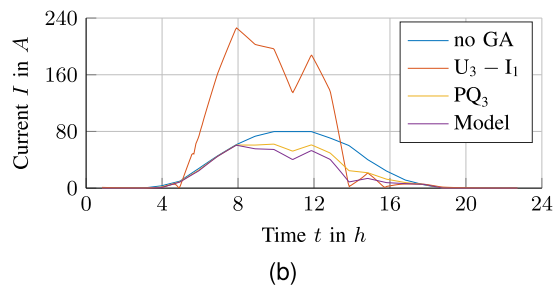
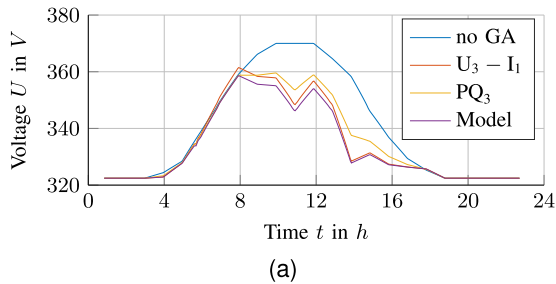


FIGURE 13. Comparison on TH1 for node cases w/o GA, $U_3 - I_1$, PQ_3 and Model for : (a) Voltage, (b) current, and (c) angle between voltage and current.

As shown in Section IV-D, two different profiles are used. One to simulate a cloudy day in the model and one with a typical sunny day as reference for the DT. In this case, the induced RRMSE between the models is 68.82%. This deviation highlights that the DT response differs greatly from the simulated “real” model in the event of unforeseen changes. The voltage discrepancy in Fig. 13(a) between the values of the Model and the DT w/o GA has an RRMSE of 3.20%, and can be appreciated how the GA configurations $U_3 - I_1$ and PQ_3 reduces it considerably down to an RRMSE of 0.43% and 1.01% respectively. Fig. 13(b) presents the current

magnitude with a large induced RRMSE of 60.39%, due to the different PV profiles that strongly affect the current injection. A counterproductive action is appreciated on the node case $U_3 - I_1$ due to the vicinity of the coupling method $U(u)$ in the node TH1 and the coupling method $I(i)$ in the node Trafo presenting an RRMSE greater than 100%, while the RRMSE with the node case PQ_3 is brought down to 24.58%. Finally, in Fig. 13(c) the angle ϕ between the Model and the DT w/o GA models shows no significant deviation with an RRMSE of 2.20%. As expected from the configuration $U_3 - I_1$ which uses coupling methods $U(u)$ and $I(i)$ where the angle is not a controlled variable, its RRMSE is greater than 100%. With the configuration PQ_3 , a positive influence on the angle can be expected thanks to the principle of the coupling method $I(u, p, q)$; the compensation of the active and reactive power at the node indirectly corrects the angle and shifts it closer to the real value. In this case, the RRMSE is reduced to 1.30%.

With the same aforementioned procedure, the RRMSE for the magnitudes of voltage and current, as well as for the angle ϕ are calculated and presented in Table 8 for all node cases shown in Table 7. The table columns represent the node cases, while the rows present each node, grouped on voltage magnitude U_{mag} , current magnitude I_{mag} and phase angle Angle ϕ . A color scale from green to red shows which values are closer or further respectively, to the simulated “real” model. If using the node case w/o GA as a base reference, a quick glance can determine that the coupling method $U(u)$ considerably reduce the error on the voltage, being suitable for static voltage stability analysis despite its counterproductive effect on current and angle. Using the same reference, the coupling method $I(i)$ can even bring the error down to 0%, making it perfectly suitable to analysis on load ability of long cables and substations regardless of its negative effect on the angle. On the other hand, the coupling method $I(u, p, q)$ gives a reduction of RRMSE on all variables and a very good correction of the angle deviation, making it a very good choice for angle and rotor stability by motor dominated nodes or in the case of end nodes with variable or non-controllable loads and generation.

V. CONCLUSION AND OUTLOOK

A. CONCLUSION

The simulation of grid sections on a real-time system is already being used in research without significant issues. But several challenges have arisen in connecting a real system

and transferring it from a pure simulation to a digital twin. As soon as unpredictable changes occur in the real system, e.g., different PV irradiation as used in this publication, it is necessary to feed measured values from the real system into the simulation of the digital twin. This requires a measurement system, presented here as a GA, to record the measurement data of the grid and a coupling method to read the data into the simulation.

Furthermore, it was identified that as soon as the real-time system can execute the simulation in real time, it does not need to have any additional requirements apart from the communication interface. The investigations have shown that a phasor model is sufficient for modelling the grid section. From the boundary conditions it could be concluded that a phasor simulation with sampling rates of 10 ms is sufficient for a digital grid twin and that the requirements for communication in a distributed grid section are achievable.

During the transfer of the *SysTec* test grid model to a DT, different coupling methods are used to connect the measuring points. The selection of the coupling methods is a challenging process and differs depending on the position in the grid of the digital twin. The investigation on the coupling methods for the DT shows that the methods have a strong influence on the behavior and accuracy of the DT. Each of the methods has its advantages and disadvantages, and their use in the model must be adapted accordingly. According to the results presented in Section IV-E and Table 8, the authors conclude:

- The coupling method $U(u)$ forces the node voltage to the real value, so that an error reduction down to 0.06% for the voltage is achieved at the node, although this has a negative effect on the error of the current and its angle at other nodes.
- The coupling method $I(i)$ used in the node case " $U_3 - I_1$ " reduces the current error at the transformer node down to 0.00% while the coupling method $U(u)$ in each test house maintains the voltage level. This negatively affects the angle ϕ and the currents in directly adjacent nodes equipped with a GA.
- Increasing the number of the GAs shows an increase of the accuracy of the controlled variable, by compromising the other ones.
- The coupling method $I(u, p, q)$ compensates the P and Q balance of the node, showing a strong correction of the voltage error of the node, indirectly minimizing the error on the angle ϕ , and positively influencing the other nodes metrics.
- Although coupling methods $U(u)$ and $I(i)$ show a stronger action on the controlled variable, the correction influence by using the coupling method $I(u, p, q)$ can be seen more effective as the error is reduced on all nodes and variables in comparison to the base DT node case "w/o GA" without GAs.

B. OUTLOOK

The following steps were identified as further development steps towards monitoring a grid section using digital twins. Firstly, the implementation of the digital twin of the *SysTec*

grid on a real-time-simulator is carried out. The influence of communication will then be analyzed. The plan is to use two RTS to calculate the DT on the first RTS and to run an emulated grid on the second RTS. In this case, the GA data will be transmitted via a real communication interface in which data loss phenomena could be analyzed. The development and realization of the GA is also being driven forward. One of the next planned tests is the integration of the GAs in the *Fraunhofer IEE SysTec* test site. The grid model is to be monitored by a DT and use the real measurement of the analyzers. The aim is to ensure that the operating points in all DT nodes correspond to the grid model with a suitable degree of accuracy. If this validation can be achieved, this method can be used in a more complex distribution grid in a later step. A field test is then planned in a distribution grid with several spatially distributed measurement systems and the implementation of a digital twin for the distribution grid.

ACKNOWLEDGMENT

The authors are responsible for the content of this publication.

REFERENCES

- [1] P. Palensky, M. Cvetkovic, D. Gusain., and A. Joseph, "Digital twins and their use in future power systems," *Digitaltwin*, no. 2, 2022, doi: [10.12688/digitaltwin.17435.2](https://doi.org/10.12688/digitaltwin.17435.2).
- [2] M. Zhou, J. Yan, and D. Feng, "Digital twin and its application to power grid online analysis," *CSEE J. Power Energy Syst.*, vol. 5, no. 3, pp. 391–398, Sep. 2019, doi: [10.17775/CSEEJPES.2018.01460](https://doi.org/10.17775/CSEEJPES.2018.01460).
- [3] N. Tomin, V. Kurbatsky, V. Borisov, and S. Musalev, "Development of digital twin for load center on the example of distribution network of an urban district," in *Proc. E3S Web Conf.*, vol. 209, 2020, Art. no. 02029, doi: [10.1051/e3sconf/202020902029](https://doi.org/10.1051/e3sconf/202020902029).
- [4] D. Gonschor, "Entwicklung der software eines messanalysators für zwillinge von verteilnetzen," Master-thesis, TH Köln Univ. Applied Sci., Cologne, Germany, 2023.
- [5] D. Gonschor, J. Steffen, J. A. M. Perez, and M. Jung, "Software development of a grid analyzer for digital twins of distribution grids," in *Proc. 2023 8th IEEE Workshop Electron. Grid (eGRID)*, 2023, pp. 1–6, doi: [10.1109/eGrid58358.2023.10380921](https://doi.org/10.1109/eGrid58358.2023.10380921).
- [6] C. Dufour, C. Andrade, and J. Bélanger, "Real-time simulation technologies in education: A link to modern engineering methods and practices," in *Proc. 11th Int. Conf. Eng. Technol. Educ. (INTERTECH 2010)*, Ilhéus, Brazil, 2010, pp. 7–10.
- [7] M. Matar and R. Irvani, "The reconfigurable-hardware real-time and faster-than-real-time simulator for the analysis of electromagnetic transients in power systems," *IEEE Trans. Power Del.*, vol. 28, no. 2, pp. 619–627, Apr. 2013.
- [8] F. Schloegl, S. Rohjans, S. Lehnhoff, J. Velasquez, C. Steinbrink, and P. Palensky, "Towards a classification scheme for co-simulation approaches in energy systems," in *2015 Int. Symp. Smart Electric Distrib. Syst. Technol. (EDST)*, Vienna, Austria, 2015, pp. 516–521, doi: [10.1109/SEDST.2015.7315262](https://doi.org/10.1109/SEDST.2015.7315262).
- [9] A. Fuller, Z. Fan, C. Day, and C. Barlow, "Digital twin: Enabling technologies, challenges and open research," *IEEE Access*, vol. 8, pp. 108952–108971, 2020, doi: [10.1109/ACCESS.2020.2998358](https://doi.org/10.1109/ACCESS.2020.2998358).
- [10] P. Kundur et al., "Definition and classification of power system stability," *IEEE Trans. Power Syst.*, vol. 19, no. 3, pp. 1387–1401, Aug. 2004.
- [11] M. A. Hannan and K. W. Chan, "Modern power systems transients studies using dynamic phasor models," *IEEE Power System Technol.*, 2004, pp. 1469–1473, vol. 2, doi: [10.1109/ICPST.2004.1460234](https://doi.org/10.1109/ICPST.2004.1460234).
- [12] M. D. O. Faruque et al., "Real-time simulation technologies for power design, testing and analysis," *IEEE Power Energy Technol. Syst. J.*, vol. 2, no. 2, pp. 63–67, Jun. 2015.
- [13] R. Brandl, "Design of a power hardware-in-the-loop capable real-time validation environment for stability analyses of electrical power system," Dissertation, Univ. Kassel, Kassel, Germany, 2018.

- [14] T. Strasser, M. Stifter, F. Andren, and P. Palensky, "Co-simulation training platform for smart grids," *IEEE Trans. Power Syst.*, vol. 29, no. 4, pp. 1989–1997, Jul. 2014, doi: [10.1109/TPWRS.2014.2305740](https://doi.org/10.1109/TPWRS.2014.2305740).
- [15] P. Palensky, A. A. v. d. Meer, C. D. Lopez, A. Joseph, and K. Pan, "Co simulation of intelligent power systems: Fundamentals, software architecture, numerics, and coupling," *EEE Ind. Electron. Mag.*, vol. 11, no. 1, pp. 34–50, Mar. 2017, doi: [10.1109/MIE.2016.2639825](https://doi.org/10.1109/MIE.2016.2639825).
- [16] L. Wright and S. Davidson, "How to tell the difference between a model and a digital twin," *Adv. Model. Simul. Eng. Sci.*, vol. 7, no. 1, 2020, Art. no. 13, doi: [10.1186/s40323-020-00147-4](https://doi.org/10.1186/s40323-020-00147-4).
- [17] F. Arraño-Vargas and G. Konstantinou, "Modular design and real-time simulators toward power system digital twins implementation," *IEEE Trans. Ind. Inform.*, vol. 19, no. 1, pp. 52–61, Jan. 2023, doi: [10.1109/TII.2022.3178713](https://doi.org/10.1109/TII.2022.3178713).
- [18] E. Glaessgen and D. Stargel, "The digital twin paradigm for future NASA and US air force vehicles," in *Proc. 53rd AIAA/ASME/ASCE/AHS/ASC Structures, Struct. Dyn. Mater. Conf. 20th AIAA/ASME/AHS Adaptive Structures Conf. 14th AIAA*, 2012, pp. 6–11, doi: [10.2514/6.2012-1818](https://doi.org/10.2514/6.2012-1818).
- [19] Y. Chen, "Integrated and intelligent manufacturing: Perspectives and enablers," *Engineering*, vol. 3, no. 5, pp. 588–595, 2017, doi: [10.1016/J.ENG.2017.04.009](https://doi.org/10.1016/J.ENG.2017.04.009).
- [20] Z. Lui, N. Meyendorf, and N. Mrad, "The role of data fusion in predictive maintenance using digital twin," in *Proc. Annu. Rev. Prog. Quant. Nonde-*, Provo, UT, USA, 2018, Art. no. 020023.
- [21] S. Boschert and R. Rosen, "Digital twin—the simulation aspect," in *Mech-atronic Futures: Challenges and Solutions for Mechatronic Systems and their Designers*, P. Hehenberger and D. Bradley, Ed. Switzerland: Springer, 2016, pp. 59–74.
- [22] I. Mathworks, "FFT: Fast Fourier transform." Accessed: Aug. 12, 2024. [Online]. Available: <https://mathworks.com/help/matlab/ref/fft.html>
- [23] P. Rodriguez, R. Teodorescu, I. Candela, A. V. Timbus, M. Liserre, and F. Blaabjerg, "New positive-sequence voltage detector for grid synchronization of power converters under faulty grid conditions," in *Proc. 37th IEEE Power Electron. Specialists Conf.*, Jeju, Korea, 2006, pp. 1–7, doi: [10.1109/PESC.2006.1712059](https://doi.org/10.1109/PESC.2006.1712059).
- [24] F. Sevilmiy and H. Karaca, "Performance enhancement of DSOGI-PLL with a simple approach in grid-connected applications," *Energy Rep.*, vol. 8, pp. 9–18, 2022, doi: [10.1016/j.egy.2021.11.186](https://doi.org/10.1016/j.egy.2021.11.186).
- [25] P. Rodriguez, A. Luna, M. Ciobotaru, R. Teodorescu, and F. Blaabjerg, "Advanced grid synchronization system for power converters under unbalanced and distorted operating conditions," in *Proc. IECON 2006-32nd Annu. Conf. IEEE Ind. Electron.*, Paris, 2006, pp. 5173–5178, doi: [10.1109/IECON.2006.347807](https://doi.org/10.1109/IECON.2006.347807).
- [26] P. Rodriguez, A. Luna, I. Candela, R. Mujal, R. Teodorescu, and F. Blaabjerg, "Multiresonant frequency-locked loop for grid synchronization of power converters under distorted grid conditions," *IEEE Trans. Ind. Electron.*, vol. 58, no. 1, pp. 127–138, Jan. 2011, doi: [10.1109/TIE.2010.2042420](https://doi.org/10.1109/TIE.2010.2042420).
- [27] S. Higginbotham, "New ethernet protocol keeps the industrial IoT in sync: Factory machines will use time-sensitive networking to coordinate their work." Accessed: Aug. 12, 2024. [Online]. Available: <https://spectrum.ieee.org/new-ethernet-protocol-keeps-the-industrial-iot-in-sync>
- [28] *IEEE Standard for Synchrophasor Data Transfer for Power Systems*, IEEE Standard C37.118.2-2011, 2011.
- [29] E. F. Arias, L. Combrinck, P. Gabor, C. Hohenkerk, and P. K. Seidelmann, "The Science of Time 2016 (Time in Astronomy and Society, Past, Present and Future 50)," Cham, Switzerland: Springer International Publishing, 2017.
- [30] D. L. Mills, "Network time protocol (version 3): Specification, implementation and analysis," *Univ. Delaware Netw. Work. Group*, 1992.
- [31] M. Sourabha and R. Shanta, "An overview of network time protocol," *R V College of Engineering, High Technol. Lett.*, vol. 27, 2021.
- [32] W. Babel, "IoT, Ethernet TCP/IP, OPC UA und cloud computing," in *Internet of Things und Industrie 4.0 (essentials)*, W. Babel, Ed. Wiesbaden, Germany: Springer Fachmedien Wiesbaden, 2023.
- [33] D. Antonic, "Ethernet communication in microcontroller systems," 2017, doi: [10.13140/RG.2.2.27380.35206](https://doi.org/10.13140/RG.2.2.27380.35206).
- [34] Siemens, "PROFINET - real-time communication in the field." Accessed: Aug. 12, 2024. [Online]. Available: <https://www.siemens.com/global/en/products/automation/industrial-communication/profinet.html>
- [35] EtherCAT Technology Group, "EtherCAT: The ethernet fieldbus." Accessed: Aug. 12, 2024. [Online]. Available: <https://www.ethercat.org/default.html>
- [36] DNP, "Overview of DNP protocol." Accessed: Aug. 12, 2024. [Online]. Available: <https://www.dnp.org/About/Overview-of-DNP3-Protocol>
- [37] Eur. Commission, "JRC photovoltaic geographical information system." [Online]. Available: https://re.jrc.ec.europa.eu/pvg_tools/en/#api_5.2
- [38] R. P. Geek, "Den energiebedarf von haushaltsgeraeten im auge behalten (seite 2). From raspberry pi geek magazine," Mar. 2023. [Online]. Available: <https://www.raspberry-pi-geek.de/ausgaben/rpg/2023/03/den-energiebedarf-von-haushaltsgeraeten-im-auge-behalten/2/#artRef-14>
- [39] Modelica Association, "Functional mock-up interface." Accessed: Aug. 12, 2024. [Online]. Available: <https://fmi-standard.org/>
- [40] S. Pavan, R. Schreier, and G. Temes, *Understanding Delta-Sigma Data Converters*, Hoboken, NJ, USA: Wiley, 2017, doi: [10.1002/9781119258308](https://doi.org/10.1002/9781119258308).
- [41] Fraunhofer IEE, "SysTec| verteilungsnetze und netzintegration". Accessed: Aug. 12, 2024. [Online]. Available: <https://www.iee.fraunhofer.de/de/testzentren-und-labore/iee-systec.html>
- [42] H. D. Kambezidis, "3.02 - The solar resource," in *Comprehensive Renewable Energy*, A. Sayigh, Ed. Amsterdam, Netherlands: Elsevier, 2012, pp. 27–84, doi: [10.1016/B978-0-08-087872-0.00302-4](https://doi.org/10.1016/B978-0-08-087872-0.00302-4).



DERK GONSCHOR was born in Bergisch Gladbach, Germany, in 1999. He received the B.Eng. degree from the Bonn-Rhein-Sieg University of Applied Sciences, Germany, and the M.Sc. degree in renewable energies from the TH Köln University of Applied Sciences, Cologne, Germany, in 2023. Parallel to his master studies, he started working as a Research Associate with the Bonn-Rhein-Sieg University of Applied Sciences, Sankt Augustin, Germany, as a Member of the Power Electronics and Power Systems Lab (PEPS-Lab), Institute

for Technology, Resource and Energy-efficient Engineering (TREE). His research interest includes topics such as real-time simulations, hardware-in-the-loop as well as digital twins.



JONAS STEFFEN was born in Lübeck, Germany, in 1986. He received the M.Sc. degree in electrical engineering from the University of Kassel, Kassel, Germany, in 2014. Since 2014, he has been a Research Associate with the Fraunhofer Institute for Energy Economics and Energy System Technology, Kassel, Germany. His current research interests include the control theory of grid-tied inverters, DC converters and electrical machines. He is also an expert in the implementation of control algorithms on DSP and FPGA. Since 2021, he

heads the Inverter Control and Embedded Systems Group and is a Senior Expert for hardware-near inverter control strategies.



JUAN ALVARO MONTOYA PEREZ born in Medellin, Colombia, in 1989. He received the Bachelor of Science degree from the Pontifical Bolivarian University, Medellin, Colombia, in 2011, and the Master of Engineering degree from the University of Applied Sciences Kempten, Kempten, Germany, in 2016. Since 2016, he has been a Research Associate with Fraunhofer IEE, Kassel, Germany, focusing on hardware-near inverter control strategies and implementation of control algorithms with the Group Inverter Control and Embedded Systems. With expertise in control technology, network

integration and stability of decentralized generation, he shows interest on hardware-in-the-loop, digital twins and advance laboratory testing methods.



CHRISTIAN BENDFELD was born in Ahaus, Germany, in 1991. He completed his studies in electrical engineering in 2019. He received the M.Sc. degree from RWTH Aachen University, Aachen, Germany. During his academic pursuits, he specialized in the control of grid-tied inverters and subsequently gained more than two years of experience in software development, SMA Solar Technology. Since 2022, he has been a part of the Fraunhofer IEE, contributing to the Converters and Drive Technology Department within the

Power Electronics Application Group. In his research, he concentrates on grid-forming control and power hardware-in-the-loop.

DETLEF NAUNDORF was born in Eisenach, Germany, in 1961. He received the degree in electrical engineering from the Technical University of Ilmenau, Ilmenau, Germany. At MicroNova AG, he is a Senior Business Development Manager for hardware in the loop test systems.

PHILIPP KOST was born in Düsseldorf, Germany, in 1983. He received degree in electrical engineering from the University of Applied Sciences, Aachen, Germany. At MicroNova AG he is working on model integration into the MicroNova NovaCarts platform.



CHRISTIAN AIGNER was born in 1968 in Wels, Austria. He was trained there as an Electrical Engineer. He has extensive knowledge of software development. He started his career with PLC programming, process visualization and industrial automation. He also developed software interfaces between ERP systems (SAP) and Geographic Information Systems (GIS). Later on he also developed navigation systems for aviation. He has been working with MicroNova as a Developer with the Testing Solutions Department since 2019 and in

Business Development since 2021. His research interests include robotic systems, Linux in its variants, FPGA and raspberry Pi.

FLORIAN FÜLLGRAF received the bachelor's degree in electrical engineering from the University of Kassel, Kassel, Germany. Florian has been with the Fraunhofer Institute for Energy Economics and Energy System Technology (IEE) as a student in a dual Student Program since 2019. The program combines an apprenticeship as an electronics technician for devices and systems.



RON BRANDL completed his studies in electrical engineering in 2010, and received the Doctorate degree in engineering from the University of Kassel, Kassel, Germany, in 2018. Since 2011, he has been a Research Associate with the Fraunhofer Institute for Energy Economics and Energy System Technology - IEE, leading the Group Power Electronics Applications. Furthermore, He has been actively engaged as a Project Manager and Researcher with the European Distributed Energy Resource Laboratories e.V. - DERLab since 2018,

where he managed the IEA TCP ISGAN-SIRFN network as German National Expert. In addition to his roles at Fraunhofer IEE and DERLab, Dr. Brandl also holds a position as a Private Lecturer with the Bonn-Rhein-Sieg University of Applied Sciences, Germany, where he imparts knowledge through laboratory courses on topics such as digital twins, rapid prototyping, and hardware-in-the-loop.



MARCO JUNG (Senior Member, IEEE) completed an apprenticeship for communication electronics in 2003 and continued to study Electrical Engineering at the TH Mittelhessen University of Applied Sciences, Giessen, Germany, and with the University of Kassel, Kassel, Germany, received the Diploma and M.Sc. degrees in 2008 and 2010, respectively, and the Ph.D. degree from the Leibniz University Hannover, Hanover, Germany, in 2016. Parallel to his Ph.D. studies, he started working with the Fraunhofer IEE in 2010. Since 2017, he

has been the Head of the Converters and Drive Technology Department. In 2019, he became a full Professor with the Bonn-Rhein-Sieg University of Applied Sciences, Sankt Augustin, Germany, and he also heads the Power Electronics and Power System-Lab. He has been the Chairman of the IEEE Joint IES/IAS/PELS German Chapter since January 1st, 2021. He is a member of the International Scientific Committee (ISC) of the European Power Electronics and Drives Association (EPE) and a member of the European Center for Power Electronics (ECPE).